CO-ASSEMBLY AND MULTICOMPONENT HYDROGEL FORMATION UPON MIXING NUCLEOBASE-CONTAINING PEPTIDES

Tristan Giraud,[a] Sabine Bouguet-Bonnet,[b] Marie-José Stébé,[c] Lionel Richaudeau,[d] Guillaume Pickaert,[a] Marie-Christine Averlant-Petit,[a] Loic Stefan*,[a]

[a] Université de Lorraine, CNRS, LCPM, F-54000 Nancy, France

[b] Université de Lorraine, CNRS, CRM2, F-54000 Nancy, France

[c] Université de Lorraine, CNRS, IJB, F-54000 Nancy, France

[d] Université de Lorraine, CNRS, L2CM, F-54000 Nancy, France

- SUPPORTING INFORMATION –

Synthesis of nucleopeptides PNA(X)-pep (X = A, T, C, G) and Aeg-pep.

Peptides were synthesized at a 400 µmol-scale both manually and on an automated ResPep XL synthesizer (Intavis AG) following an already reported protocol (T. Giraud *et al*., *Nanoscale*, **2020**, *12*, 19905-19917). Briefly, using a Fmoc/^{t}Bu strategy, standard experimental conditions for each coupling were: Fmoc-amino acid / 2-(1*H*-benzotriazol-1-yl)-1,1,3,3-tetramethyl-uronium tetrafluoroborate (HBTU) / 4-methylmorpholine (NMM) at 6 / 5 / 10 equivalents (double coupling, 2 x 40 min), or Fmoc-PNA-G(Bhoc)-OH, PNA-A(Bhoc)-OH, Fmoc-PNA-C(Bhoc)-OH, Fmoc-PNA-T-OH / HBTU / NMM at 3 / 3 / 6 equivalents (double coupling, 2 x 3 hours). Fmoc-deprotection steps were carried out using a 20% piperidine solution in DMF, and final cleavages were achieved using a trifluoroacetic acid/triisopropylsilane/water (92,5/5/2,5) mixture. The crude peptides were precipitated from cold diethylether (-20 °C), centrifuged, washed with cold diethylether, dried under reduced pressure, resolubilized in water and finally, lyophilized. Then, peptides were purified by reversed-phase semi-preparative HPLC (Waters 600 HPLC System) equipped with a Nucleosil (Macherey-Nagel) 100-5 C_{18} 250×21 mm column. The resulting solutions were evaporated under reduced-pressure and double-lyophilized. The purity of each peptide was evaluated by analytical reversed-phase HPLC (Shimadzu Prominence UFLC) equipped with a Nucleosil (Macherey-Nagel) 100-5 C_{18} 250×4.6 mm column and coupled with a mass spectrometer (Shimadzu LCMS2020).

	6 hours	3 months	6 months
Aeg-pep	Solution	Solution	Solution
PNA(C)-pep	Solution	Solution	Solution
PNA(T)-pep	Solution	Solution	Solution
PNA(A)-pep	Translucent **gel**	Translucent **gel**	Translucent **gel**
PNA(G)-pep	Translucent **gel**	Translucent **gel**	Translucent **gel**
PNA(A)-pep + PNA(T)-pep	Translucent **gel**	Translucent **gel**	Translucent **gel**
PNA(A)-pep + Aeg-pep	Clear **gel**	Translucent **gel**	Translucent **gel**
PNA(T)-pep + Aeg-pep	Clear **gel**	Clear **gel**	Clear **gel**
PNA(G)-pep + PNA(C)-pep	Translucent **gel**	Translucent **gel**	Translucent **gel**
PNA(G)-pep + Aeg-pep	Clear **gel**	Translucent **gel**	Translucent **gel**
PNA(C)-pep + Aeg-pep	Solution	Solution	Clear **gel** (*very weak*)

Table S1 – Evolution of the macroscopic visual aspect of each sample after 6 hours, 3 and 6 months.

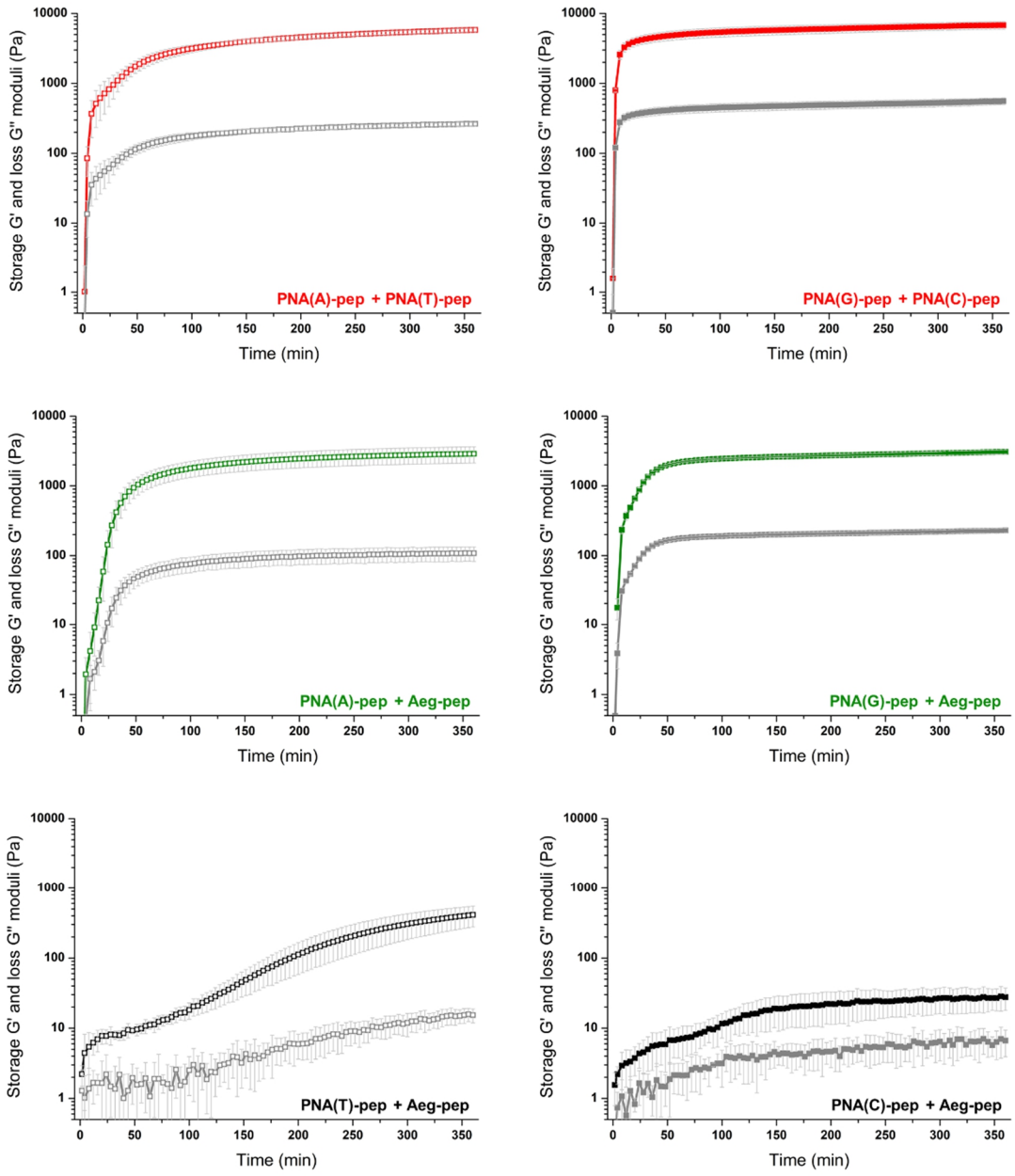

Figure S1 – Time sweep rheological data (G' in color or black, G'' in grey). All the experiments were carried out at 7.5mM of each compound in Tris.HCl (1 M, pH 7.4).

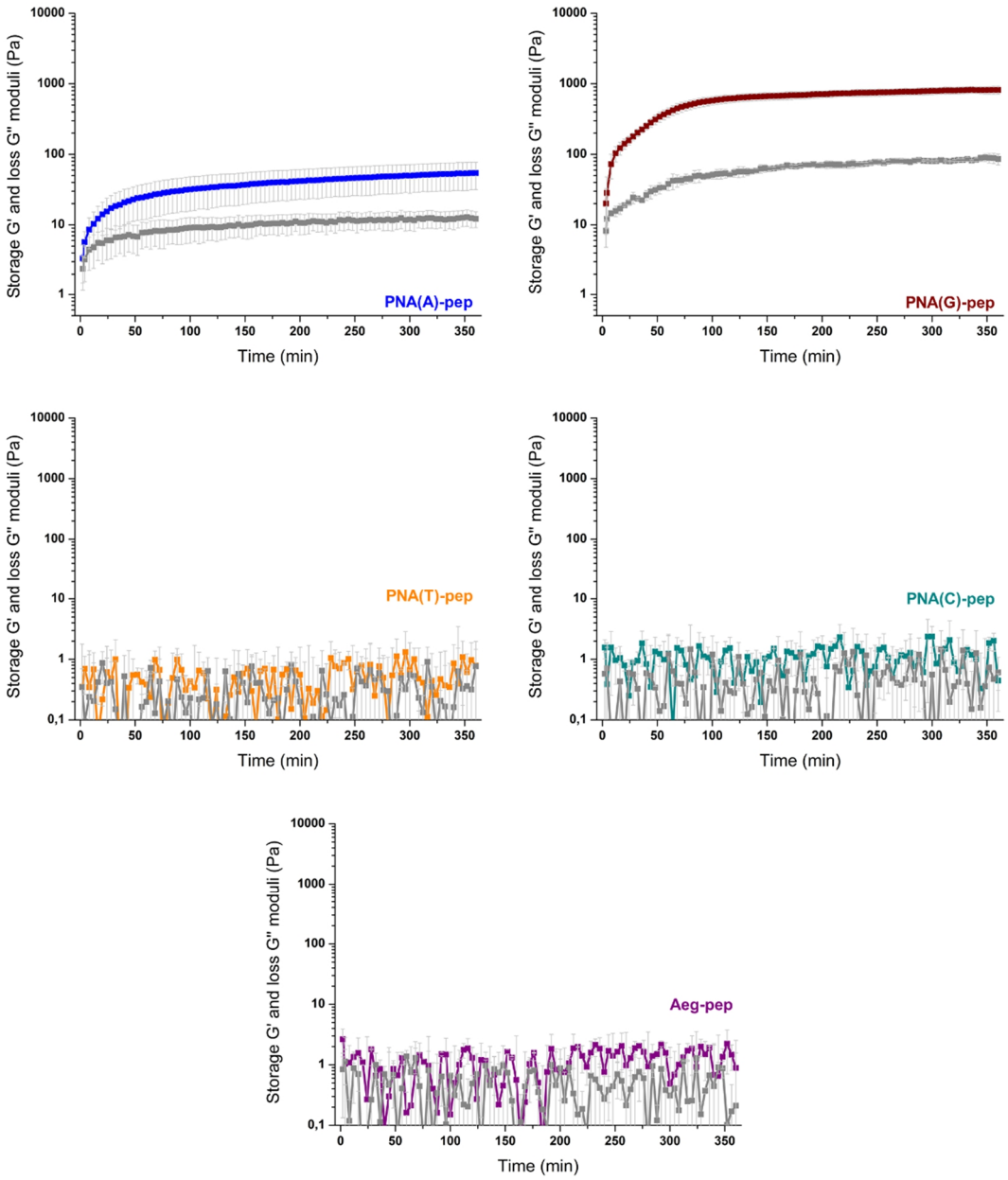

Figure S2 – Time sweep rheological data (G' in color, G'' in grey). All the experiments were carried out at 7.5 mM of each compound in Tris.HCl (1 M, pH 7.4).

	Sol/gel transition time $t_{s/g}$	Macroscopic aspect	Gelification time t_{gel}	Storage modulus G' (Pa)	Loss modulus G'' (Pa)	Yield point τ_y (Pa)	Initial stiffening rate V_0 (Pa.min^{-1})
Aeg-pep	*n.d.*	Solution	*n.d.*	**1.5** (dev. std. 0.6)	**0.1** (dev. std. 0.1)	**< 1**	*n.d.*
PNA(C)-pep	*n.d.*	Solution	*n.d.*	**0.9** (dev. std. 0.2)	**0.5** (dev. std. 0.1)	**< 1**	*n.d.*
PNA(T)-pep	*n.d.*	Solution	*n.d.*	**0.5** (dev. std. 0.1)	**0.3** (dev. std. 0.1)	**< 1**	*n.d.*
PNA(A)-pep	**70 min** (±10 min)	Translucent gel	**> 360 min**	**54.5** (dev. std. 22.9)	**12.2** (dev. std. 3.1)	**< 1**	**1.39** (dev. std. 0.18)
PNA(G)-pep	**13 min** (±3 min)	Translucent gel	**226 min** (±12 min)	**820** (dev. std. 105)	**85.9** (dev. std. 15.1)	**5.05** (dev. std. 0.35)	**7.46** (dev. std. 0.15)

Table S2 - Characteristic macroscopic and rheological properties of each compound alone at 7.5 mM in Tris.HCl (1 M, pH 7.4).

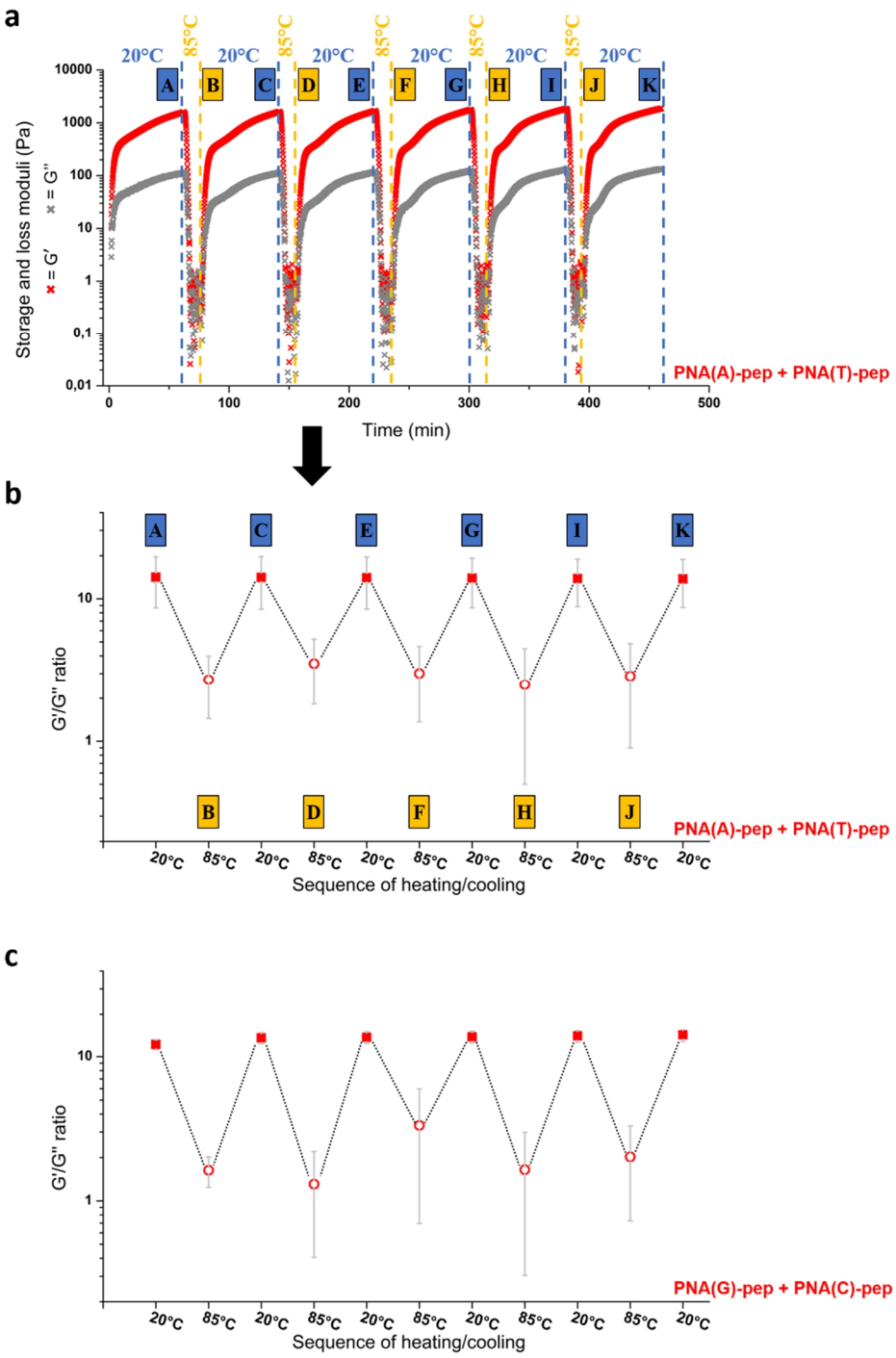

Fig S3 – (a) Illustration of the methodology used to build the graph G'/G'' as a function of the sequence of heating/cooling, and thermal recovery rheological data for (b) PNA(A)-pep + PNA(T)-pep and (c) PNA(G)-pep + PNA(C)-pep mixtures. Total concentration = 15 mM in Tris.HCl (1 M, pH 7.4).

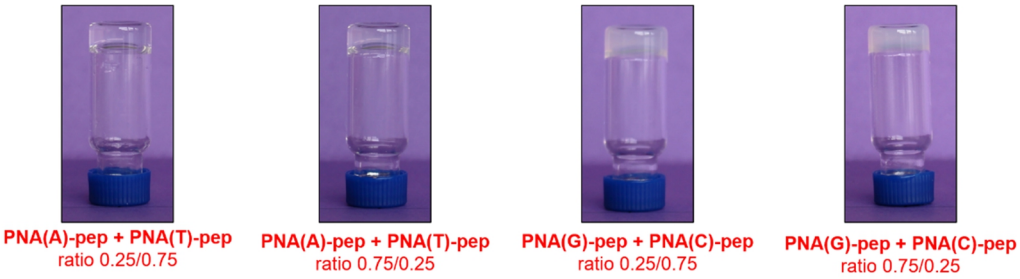

Fig S4 – Pictures of the hydrogels formulated from PNA(A)-pep + PNA(T)-pep and PNA(G)-pep + PNA(C)-pep at ratio 0.25/0.75 and 0.75/0.25. Total concentration = 15 mM in Tris.HCl (1 M, pH 7.4).

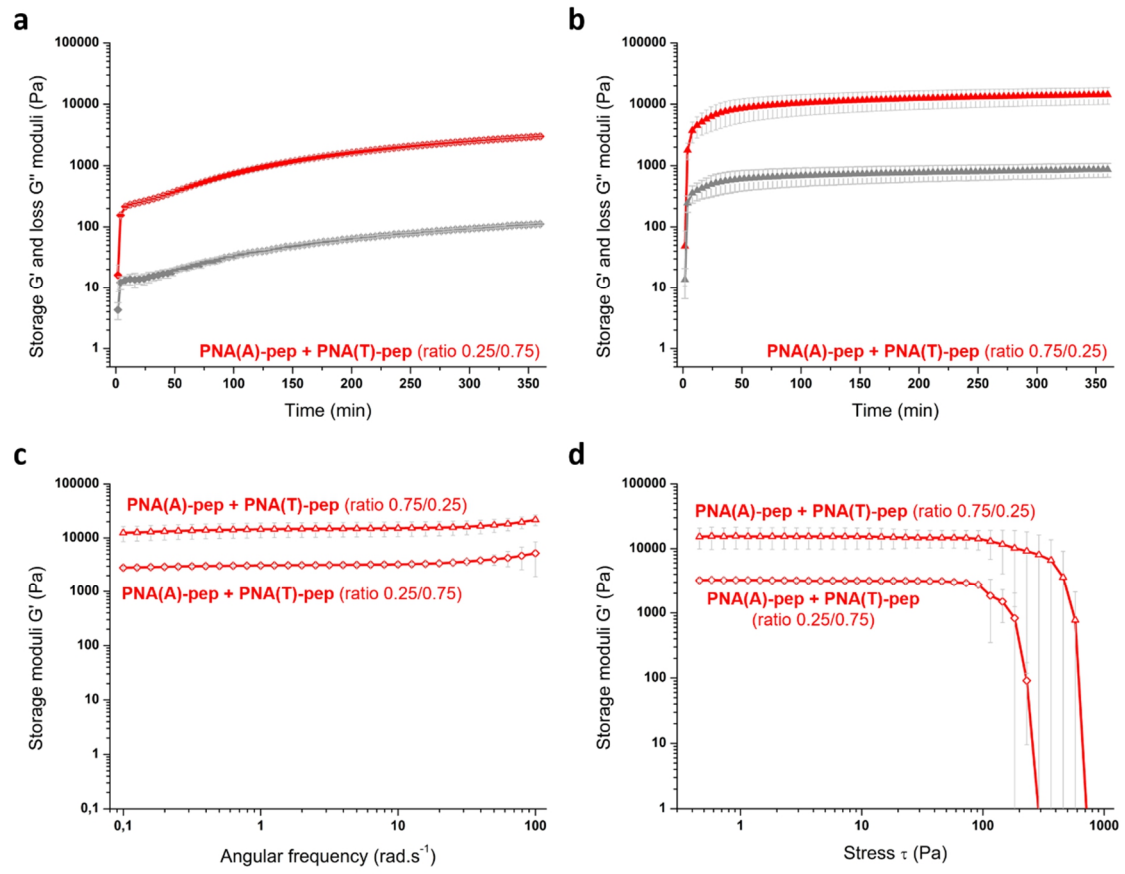

Fig S5 – (a,b) Time sweep (G' in red, G'' in grey), (c) frequency sweep and (d) stress sweep. rheological data for mixtures of PNA(A)-pep + PNA(T)-pep at ratio 0.25/0.75 and 0.75/0.25. Total concentration = 15 mM in Tris.HCl (1 M, pH 7.4).

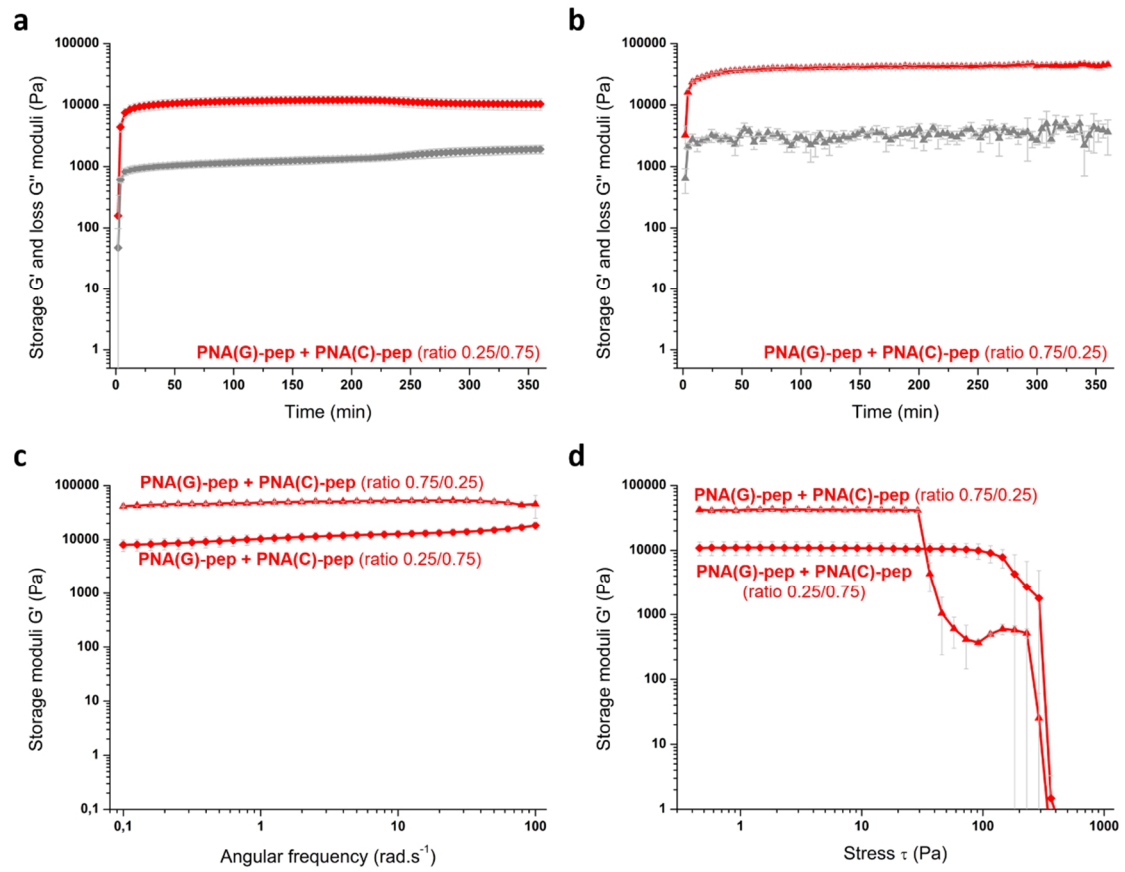

Fig S6 - (a,b) Time sweep (G' in red, G'' in grey), (c) frequency sweep and (d) stress sweep. rheological data for mixtures of PNA(G)-pep + PNA(C)-pep at ratio 0.25/0.75 and 0.75/0.25. Total concentration = 15 mM in Tris.HCl (1 M, pH 7.4).

	Sol/gel transition time $t_{s/g}$	Macroscopic aspect	Gelification time t_{gel}	Storage modulus G' (Pa)	Loss modulus G'' (Pa)	Yield point τ_y (Pa)	Initial stiffening rate V_0 (Pa.min^{-1})
PNA(A)-pep + PNA(T)-pep (ratio 0.25/0.75)	**3 min** (±2 min)	Clear gel	**> 360 min**	**2955** (dev. std. 121)	**110** (dev. std. 3.9)	**71.0** (dev. std. 5.7)	**35.4** (dev. std. 2.6)
PNA(A)-pep + PNA(T)-pep (ratio 0.75/0.25)	**5 min** (±1 min)	Translucent gel	**51 min** (±8 min)	**14296** (dev. std. 4376)	**863** (dev. std. 222)	**98.4** (dev. std. 3.6)	**521** (dev. std. 182)
PNA(G)-pep + PNA(C)-pep (ratio 0.25/0.75)	**3 min** (±1 min)	Translucent gel	**22 min** (±2 min)	**10381** (dev. std. 2185)	**1902** (dev. std. 292)	**96.5** (dev. std. 10.2)	**1128** (dev. std. 195)
PNA(G)-pep + PNA(C)-pep (ratio 0.75/0.25)	**3 min** (±1 min)	Translucent gel	**110 min** (±10 min)	**45027** (dev. std. 5658)	**3455** (dev. std. 596)	**30.5** (dev. std. 1.1)	**3853** (dev. std. 305)

Table S3 - Characteristic macroscopic and rheological properties of the mixtures comprised of PNA(A)-pep + PNA(T)-pep and PNA(G)-pep + PNA(C)-pep at ratio 0.25/0.75 and 0.75/0.25. Total concentration = 15 mM in Tris.HCl (1 M, pH 7.4).

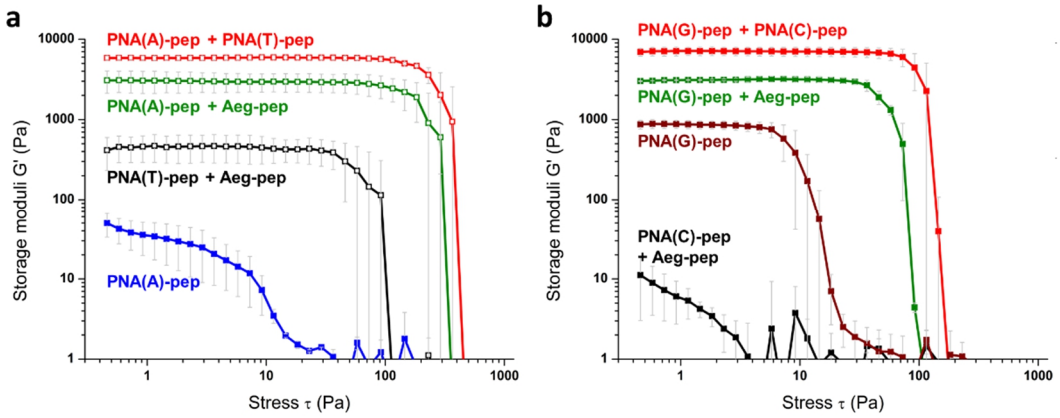

Figure S7 - Stress sweep rheological data. All the experiments were carried out at 7.5 mM of each compound in Tris.HCl (1 M, pH 7.4).

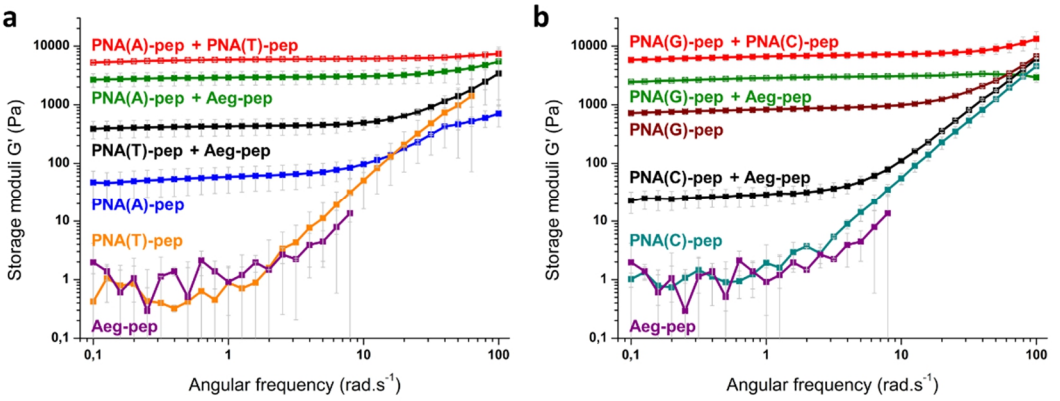

Figure S8 - Frequency sweep rheological data. All the experiments were carried out at 7.5 mM of each compound in Tris.HCl (1 M, pH 7.4).

	A(0) (s^{-1})	A(1) (s^{-1})	$\tau_c(1)$ (s)	A(2) (s^{-1})	$\tau_c(2)$ (s)	$r_1 = \frac{A(1)}{\tau_c(1)}$ (s^{-2})	$r_2 = \frac{A(2)}{\tau_c(2)}$ (s^{-2})	$\frac{r_2}{r_1 + r_2}$
PNA(A)-pep + PNA(T)-pep	0.54	0.51	7.07×10^{-8}	6.55	6.48×10^{-6}	7.21×10^{6}	1.01×10^{6}	12.3 %
PNA(A)-pep + Aeg-pep	0.54	0.33	6.28×10^{-8}	3.72	6.72×10^{-6}	5.22×10^{6}	0.554×10^{6}	9.6 %
PNA(T)-pep + Aeg-pep	0.54	0.28	6.25×10^{-8}	3.01	6.54×10^{-6}	4.54×10^{6}	0.460×10^{6}	9.2 %
PNA(G)-pep + PNA(C)-pep	0.54	0.65	7.79×10^{-8}	9.06	7.34×10^{-6}	8.35×10^{6}	1.23×10^{6}	12.8 %
PNA(G)-pep + Aeg-pep	0.54	0.46	6.04×10^{-8}	6.13	6.26×10^{-6}	7.69×10^{6}	0.979×10^{6}	11.3 %
PNA(C)-pep + Aeg-pep	0.54	0.19	4.95×10^{-8}	1.78	6.70×10^{-6}	3.87×10^{6}	0.266×10^{6}	6.4 %

Table S4 – Numeric values of the best fits obtained with a sum of Lorentzian functions $R_1(\nu_H) = A(0) + \sum_i \frac{A(i)}{1+(2\pi\nu_H\ \tau_c\ (i))^2}$ where τ_c is the correlation time describing the water motion. The proportion of water experiencing very slow motion (last column) was obtained by comparing the weight of the lorentzians $r_i = \frac{A(i)}{\tau_c(i)}$. All the experiments were carried out at a total concentration of 15 mM (*i.e.*, 7.5 mM of each compound) in Tris.HCl (1 M, pH 7.4).

	Exponent *n*	Exponent *m*	Correlation lenght *L* (nm)	A (a.u.)	C (10^{-3} a.u.)	B (10^{-3} a.u.)	$\chi 2$
PNA(A)-pep + PNA(T)-pep	1.71	1.89	9.32	4.55	18.06	1.00	0.0072
PNA(A)-pep + Aeg-pep	1.05	1.75	10.2	2.33	2.07	30.83	0.0062
PNA(T)-pep + Aeg-pep	1.02	1.51	9.02	1.40	0.97	0,0011	0.0057
PNA(G)-pep + PNA(C)-pep	1.95	2.99	9.91	19.9	10.38	0.028	0.0199
PNA(G)-pep + Aeg-pep	1.95	2.93	8.82	8.81	0.01	19.99	0.0115
PNA(C)-pep + Aeg-pep	0.99	0.71	15.0	0.43	0.05	0.0013	0.0029

Table S5 – Parameters obtained from the fitting of the SAXS data.

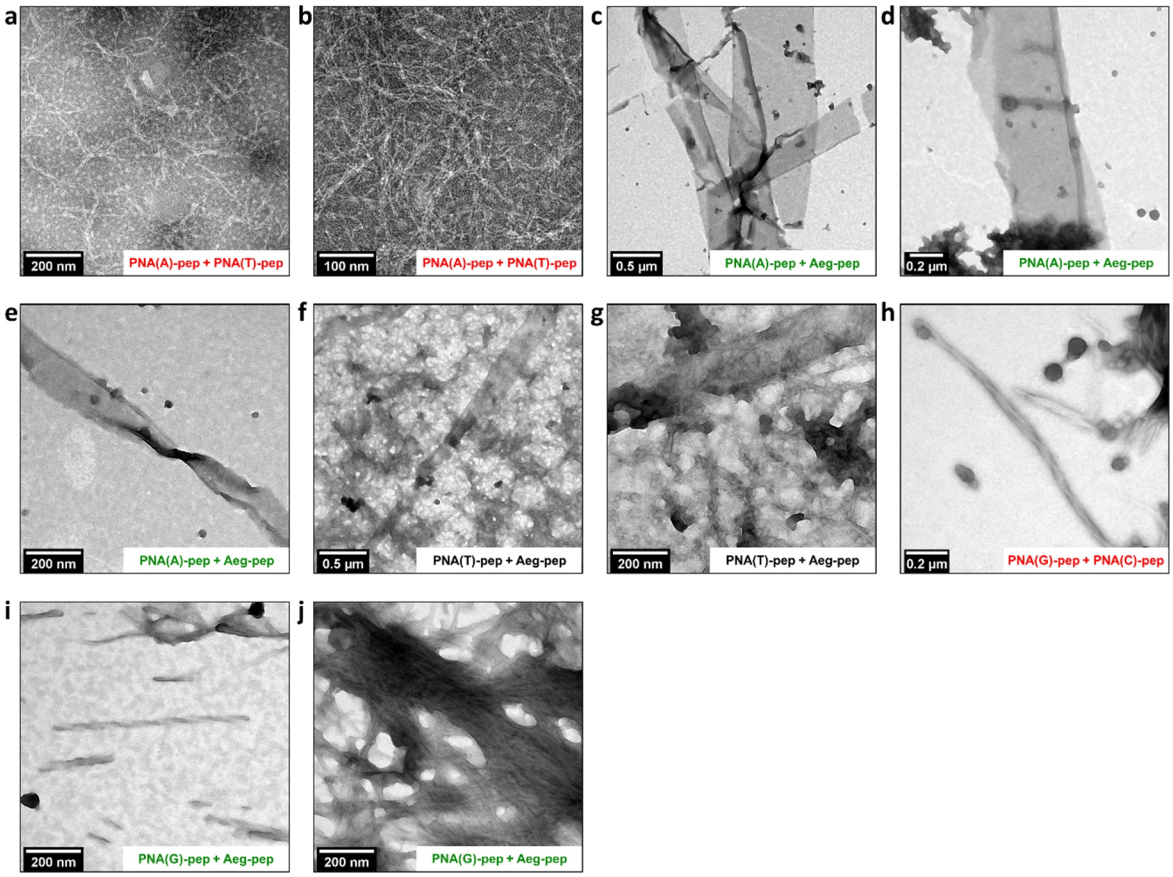

Figure S9 - TEM images of all the six multicomponent systems recorded with negative staining by phosphotungstic acid.

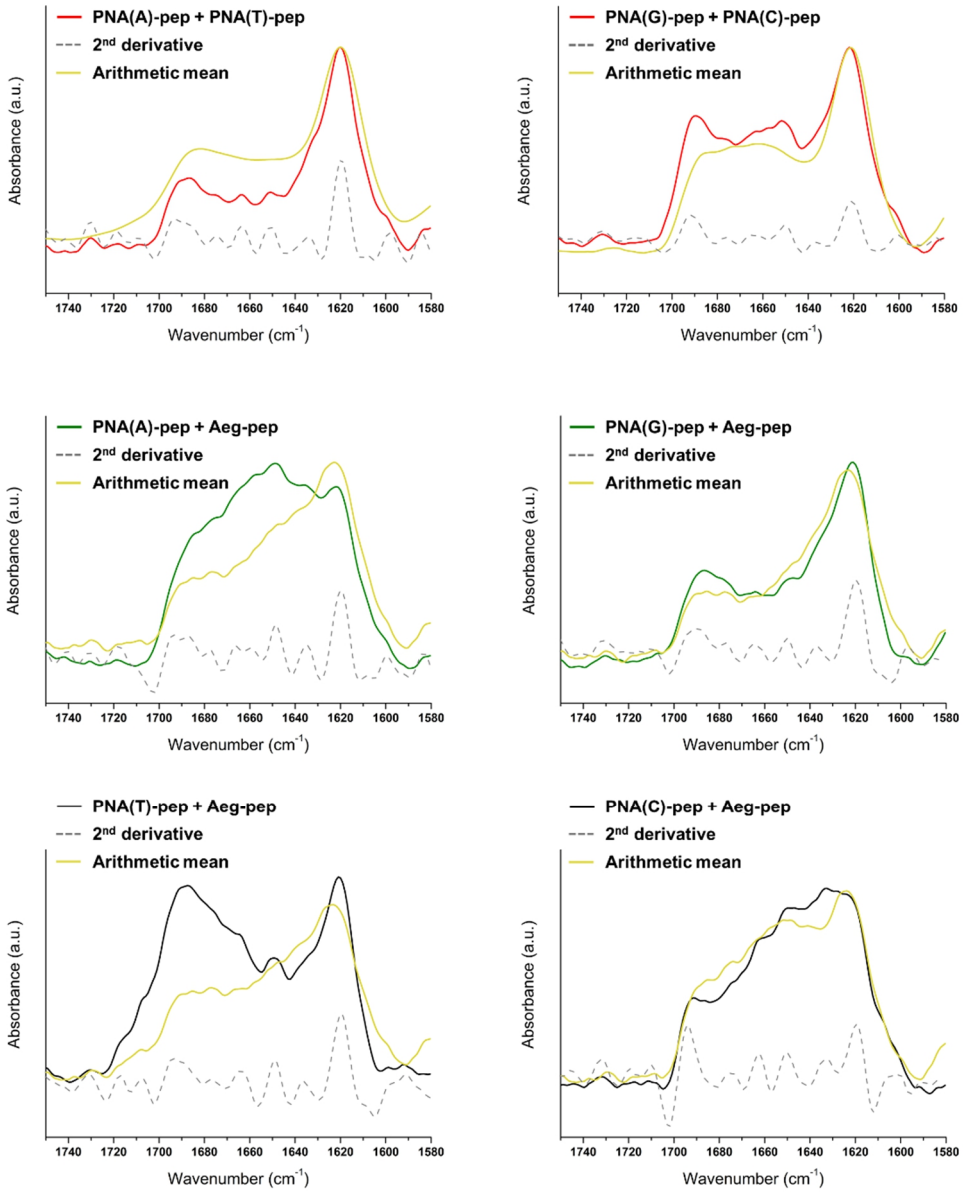

Figure S10 - FTIR spectra of the amide I region recorded at a total concentration of 15 mM (*i.e.*, 7.5 mM of each compound) in Tris.HCl (1 M, pH 7.4). *Nota*: *arithmetic mean* stands for the arithmetic mean of each nucleopeptide spectrum. Depending on the considered blend, the FTIR absorbance profiles exhibit few differences which can be correlated with observations from TEM. For instance, while **PNA(A)-pep** + **PNA(T)-pep** has a clear well defined anti-parallel β-sheet FTIR signature consistent with the homogeneous fibers observed in TEM, **PNA(A)-pep** + **Aeg-pep** and **PNA(T)-pep** + **Aeg-pep** spectra have a broad unresolved absorbance region from 1630 to 1680 cm^{-1} which can be attributed to the presence of disordered peptide structures (see L. J. Juszczak, *J. Biol. Chem*., 2004, **279**, 7395-7404), leading to more heterogeneous nano-objects (see TEM images, Fig. 6). This broad peak is also noticed for **PNA(C)-pep** + **Aeg-pep** which also forms heterogenous assemblies including ribbons or aggregates. Moreover, for each multicomponent system, we compared the measured absorbance of all the mixtures with the arithmetic mean of each constituting compound: interestingly, the two profiles do not significantly overlap meaning that in each mix, compounds are not self-sorted but co-assembled (see E. R. Draper and D. J. Adams, *Chem. Soc. Rev.*, 2018, **47**, 3395-3405), as discussed in the main manuscript.

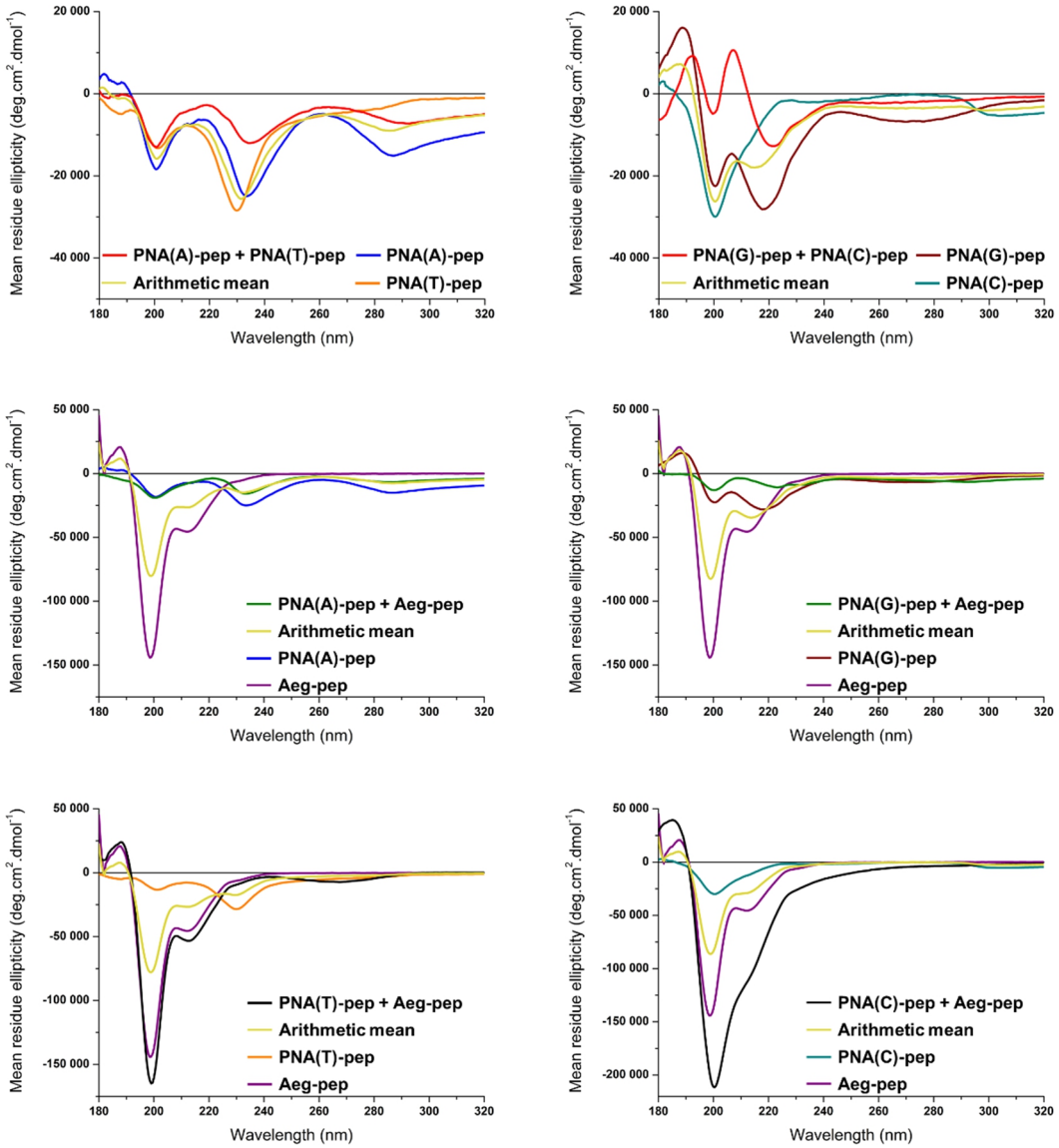

Figure S11 - Circular dichroism spectra recorded at a total concentration of 10 mM in NaF (0.67 M, pH 7.4). *Nota*: *arithmetic mean* stands for the arithmetic mean of each nucleopeptide spectrum.

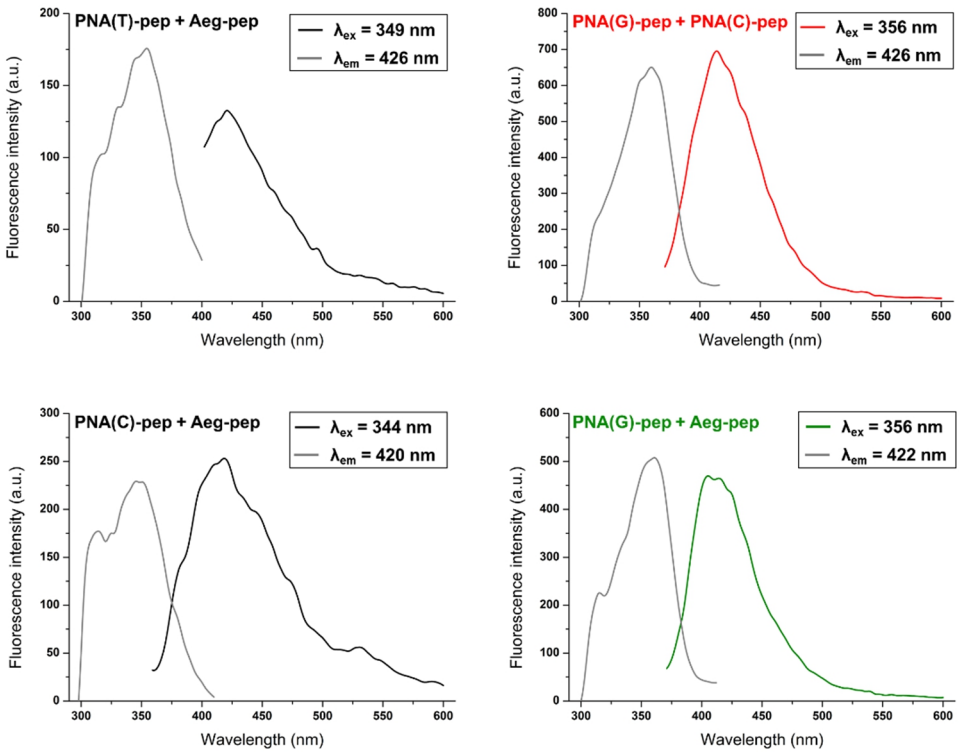

Figure S12 - Fluorescence emission and excitation spectra exhibiting a main emission peak with a maximum emission in the 400-420 nm range, and two main excitation peaks around 345-351 nm attributed to Phe/Phe interactions and at 306-315 nm attributed to nucleobase/nucleobase interactions. All the experiments were carried out at 7.5 mM of each compound in Tris.HCl (1M, pH 7.4).

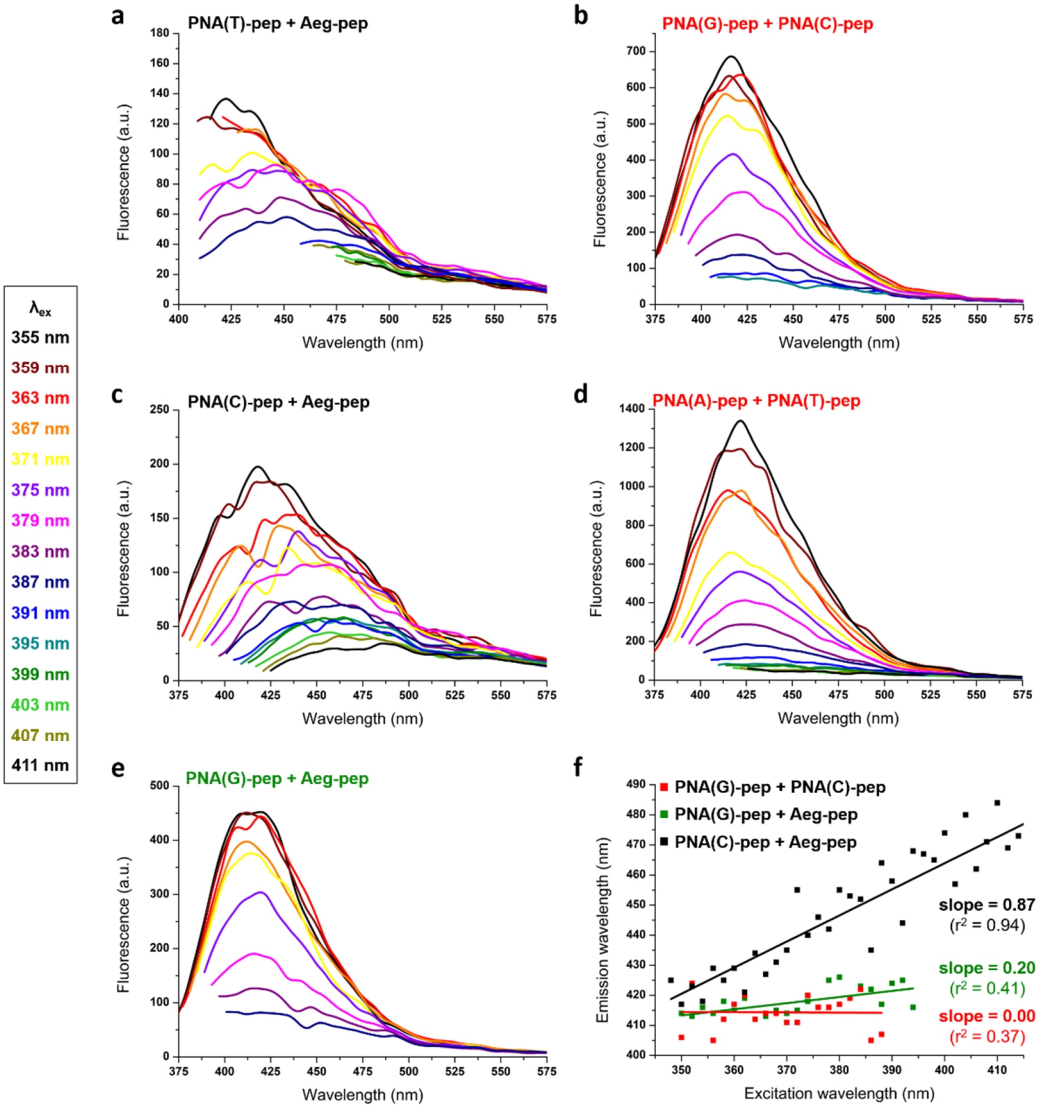

Figure S13 – (a-e) Evolution of the fluorescence emission spectra at different excitation wavelengths. (f) Plot of the linear correlations between emission and excitation wavelengths exhibiting a red-edge excitation shift (REES), and corresponding regression slopes and r^2 values for multicomponent systems comprised of PNA(G)-pep, PNA(C)-pep and/or Aeg-pep. All the experiments were carried out at 7.5 mM of each compound in Tris.HCl (1M, pH 7.4).

	Maximum intensity (a.u.)	**Lag time** (min)	k_{app} (h^{-1})
PNA(A)-pep	**50.3** (dev. std. 4.8)	**75.0** (dev. std. 6.0)	**7.78** (dev. std. 0.55)
PNA(T)-pep	**0.61** (dev. std. 0.17)	*n.d.*	*n.d.*
PNA(G)-pep	**24.2** (dev. std. 3.1)	**27.8** (dev. std. 3.0)	**5.87** (dev. std. 0.77)
PNA(C)-pep	**0.54** (dev. std. 0.15)	*n.d.*	*n.d.*
Aeg-pep	**0.75** (dev. std. 0.14)	*n.d.*	*n.d.*

Table S6 – Characteristic maximum intensities, lag time (t_{lag}) and apparent constants (k_{app}) reported for all the monocomponent samples (7.5 mM in Tris.HCl (1M, pH 7.4).